Improving the Point Spread Function of an Aberrated 7-Mirror Segmented Reflecting Telescope using a Spatial Light Modulator

Mary Angelie Alagao, Mary Ann Go, Maricor Soriano and Giovanni Tapang
National Institute of Physics, University of the Philippines, Diliman, Quezon City, Philippines

Keywords: Point Spread Function, Segmented Reflecting Telescope, Gerchberg-Saxton, Phase Retrieval.

Abstract: We reduce the aberrations in a segmented reflecting telescope composed of seven identical concave mirrors by correcting the point spread functions (PSFs) using a a spatial light modulator. We first calculate and compare the PSF of a segmented reflecting telescope and a monolithic reflecting telescope, both having the same aperture diameter. We simulate the aberrations using the Zernike polynomials and add these to the PSF of the segmented mirror. Using the Gerchberg-Saxton (GS) algorithm, we retrieve the phase information used to correct for these aberrations. Results show an improvement in the imaging resolution of the telescope due to the correction phase applied.

1 INTRODUCTION

The quest to see far into space has led to the construction of meter-wide ground-based telescopes. Increasing the aperture of a telescope increases its light gathering power, thus, allowing the detection of faint astronomical objects. A smaller angular resolution is also achieved with a larger aperture diameter as shown in Equation 1, where λ is the wavelength and D is the aperture diameter.

$$\Theta = \frac{\lambda}{D} \tag{1}$$

There is a technological limit of 10 m in the construction of large single mirror telescopes due to the cost of building and transportation of a very large mirror (G. Chanan, 2013).The solution proposed to this problem is the segmented mirror design (G. Chanan, 2013). Small mirrors are put together to act as a single large mirror. Each mirror has a specific shape and a control system for precise positioning to reduce, if not eliminate, the optical path difference between segments. While this poses structural complexity due to the control system of each segment, this solution is less expensive compared to the construction of one very large mirror, making it easier to increase the aperture diameter of a telescope.

A telescope is a diffraction-limited system. Its imaging performance can be evaluated by calculating its point spread function (PSF). The image produced by an optical system is just the Fourier transform of the aperture at the exit pupil.

Most telescopes assume a circular opening and the image of a point due to diffraction effects is the PSF. The transverse size of the PSF shows the image of a point in the image plane. The diameter of the first dark ring of PSF, known as the Airy disk, gives a measure of the resolution and its size is the smallest size that the telescope can detect (Goodman, 2005). The effective PSF detected by a camera, however, may include aberrations from imperfect alignment. The wavefront can be corrected by getting the phase information based on the difference between the aberrated PSF and the ideal PSF.

In this work, we perform numerical simulations to characterize a segmented reflecting telescope composed of seven identical concave mirrors. We intentionally add aberrations and use a spatial light modulator (SLM) to shape the wavefront in order to improve the PSF.

2 METHODOLOGY

For the segmented reflecting telescope, we used seven identical mirrors with a diameter of 76mm and a focal length 300mm. The mirrors are rotated and translated such that they focus at one point. The effective diameter of the segmented mirror is 223.22 mm. We compare our results with a monolithic reflecting telescope. For performance comparison, we denote the

Alagao, M., Go, M., Soriano, M. and Tapang, G.
Improving the Point Spread Function of an Aberrated 7-Mirror Segmented Reflecting Telescope using a Spatial Light Modulator.
DOI: 10.5220/0005691900940101
In *Proceedings of the 4th International Conference on Photonics, Optics and Laser Technology (PHOTOPTICS 2016)*, pages 96-103
ISBN: 978-989-758-174-8

monolithic reflecting telescope has the same aperture diameter as the segmented telescope. The setup of the whole system is shown in Figure 1.

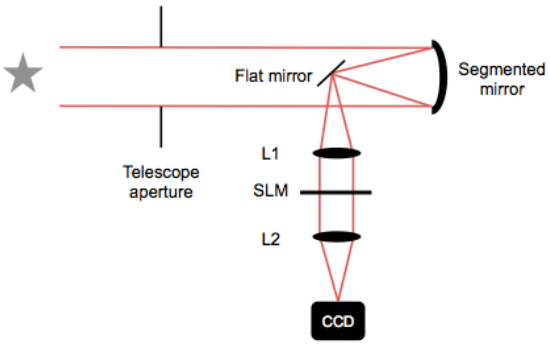

Figure 1: Optical setup for wavefront correction.

2.1 PSF Calculation

We simulate the performance of a segmented reflecting telescope using the angular spectrum method. We represent a plane wave located at z = 0 as U(x,y,0). The angular spectrum $\mathcal{U}(fx, fy, 0)$ at this location is just the Fourier transform of U(x,y,0) given by Equation 2 (Goodman, 2005).

$$\mathcal{U}(f_x, f_y; 0) = \int_{-\infty}^{\infty}\int U(x,y,0)exp[-j2\pi\phi]dxdy \quad (2)$$

where

$$\phi = f_X x + f_Y y \quad (3)$$

To get the field amplitude U(x,y,0), we get the inverse Fourier transform as shown in Equation 4.

$$U(x,y,0) = \mathcal{F}^{-1}\{\mathcal{U}(f_x, f_y; 0)\} \quad (4)$$

Similarly, the angular spectrum at a distance z is given by Equation 5.

$$\mathcal{U}(f_X, f_Y; z) = \int_{-\infty}^{\infty}\int U(x,y,z)exp[-j2\pi\phi)]dxdy \quad (5)$$

where the amplitude U(x,y,z) at a distance z is also given by

$$U(x,y,z) = \mathcal{F}^{-1}\{\mathcal{U}(f_x, f_y; z)\} \quad (6)$$

Comparing Equations 2 and 5, the relation between $\mathcal{U}(x,y,0)$ and $\mathcal{U}(x,y,z)$ is given by Equation 7.

$$\mathcal{U}(x,y,z) = \mathcal{U}(x,y,0)exp(j2\pi\sqrt{1 - f_X^2 - f_Y^2}z) \quad (7)$$

The angular spectrum methods gives us the PSF at the point (x,y,z);

2.2 Angular Spectrum of the Segmented Mirrors

The apertures, which are actually the mirrors, are as shown in Figure 2.

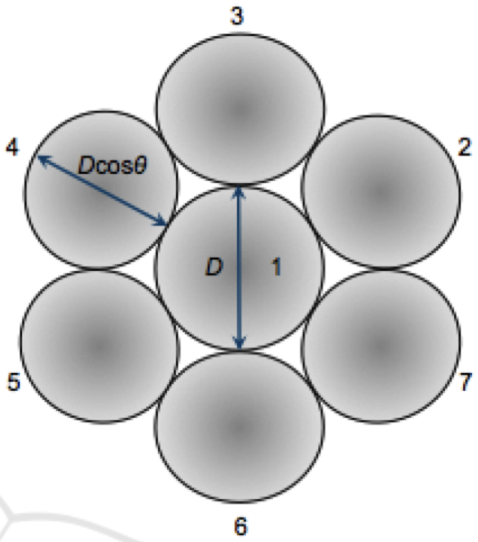

Figure 2: Top view of the configuration of the seven mirror segments where D is the diameter of the mirror segment which is equal to 76mm and θ is the tilt angle.

To simulate the PSF of this configuration, the other mirrors are rotated along the x and y axis with respect to Mirror 1, which is centered at the origin.

Each mirror must be tilted such that all the foci of the mirrors coincide. The geometry for determining the tilt angle is shown in Figure 3.

We use the sine law in △ABC to obtain the following relation:

$$\frac{d}{sin\theta} = \frac{f}{sin(90 - \frac{\theta}{2})} \quad (8)$$

Using △CBD, the left hand side in Equation 8 can be written as

$$\frac{d}{sin(180 - \theta)} = \frac{r}{sin(\frac{\theta}{2})} \quad (9)$$

Using Equation 9 in Equation 8, we get the following relation:

$$\frac{f}{cos(\frac{\theta}{2})} = \frac{r}{sin(\frac{\theta}{2})} \quad (10)$$

such that the tilt angle can now be expressed as:

$$\theta = 2tan^{-1}(\frac{r}{f}) \quad (11)$$

This was used to construct the rotation matrices for each mirror. The angle is found to be 14.4°.Setting

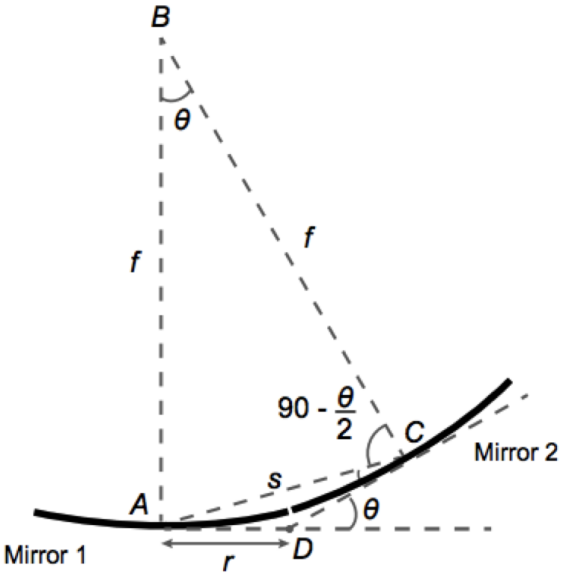

Figure 3: Geometry for determining the tilt angle of mirrors.

the optical axis along z, we use the angle to rotate about the y-axis then the x-axis depending on the position of the mirror.

$$R_{xy}(\alpha,\beta) = \begin{pmatrix} \cos\beta & \sin\alpha\sin\beta & \cos\alpha\sin\beta \\ 0 & \cos\alpha & -\sin\alpha \\ -\sin\beta & \sin\alpha\cos\beta & \cos\alpha\cos\beta \end{pmatrix} \tag{12}$$

The rotation and translation matrices given by Equations 12 and 14, respectively, were used to obtain the x and y coordinates of the off-axis mirrors as shown in Equation 13. The angles α and β are both equal to θ. The variables, dx and dy, are the translations along the x and y axes, respectively. For the diagonal mirrors, Mirror 2,4,5 and 7, dx is equal to $\sqrt{3}r\cos(\theta)$ and dy is equal to $r\cos(\theta)$.

$$\begin{pmatrix} x' \\ y' \\ z' \end{pmatrix} = T_{xy}R_{xy} \begin{pmatrix} x \\ y \\ z \end{pmatrix} \tag{13}$$

$$T_{xy} = \begin{pmatrix} 1 & 0 & dx \\ 0 & 0 & dy \\ 0 & 0 & 1 \end{pmatrix} \tag{14}$$

2.3 Aberration Simulations

Aberrations are deviations in the wavefront which reduce the intensity and contrast of an image. They can be described in terms of Zernike polynomials which are orthogonal over a unit circle.

Using the Zernike polynomials, the aberration function can be expressed in terms of polynomials as shown in Equation 18 (Mahajan, 1994).

$$W(\rho,\theta) = \sum_{j=1}^{\infty} a_j Z_j(\rho,\theta) \tag{15}$$

where the polynomial ordering number is given by j, a_j is the aberration coefficient and

$$Z_{evenj}(\rho,\theta) = \sqrt{(2n+1)}R_n^m(\rho)cosm\theta \quad m \neq 0 \tag{16a}$$

$$Z_{oddj}(\rho,\theta) = \sqrt{(2n+1)}R_n^m(\rho)sinm\theta \quad m \neq 0 \tag{16b}$$

$$Z_j(\rho,\theta) = \sqrt{(n+1)}R_n^0(\rho) \quad m = 0 \tag{16c}$$

and

$$R_n^m(\rho) = \sum_{s=0}^{(n-m)/2} \frac{(-1)^s(n-s)!}{s!(\frac{n+m}{2}-s)!(\frac{n-m}{2}-s)!} \tag{17}$$

We used the following aberrations: coma, astigmatism, spherical aberration and defocus. We simulate the aberrations using Equation 18.

$$PSF_{aberrated} = \mathcal{F}\{\mathcal{F}^{-1}\{PSF_{segmented}\}exp(i\frac{2\pi}{\lambda}\Phi)\}\} \tag{18}$$

where Φ is given by the following Zernike polynomials (M. Born, 1999)

$$\Phi_{sphericalaberration} = 5\lambda\rho^4 \tag{19}$$

$$\Phi_{coma} = 0.3\lambda\rho^3\cos\theta \tag{20}$$

$$\Phi_{astigmatism} = 10\lambda\rho^2\cos 2\theta \tag{21}$$

$$\Phi_{defocus} = 8\sqrt{(3)}(2\rho^2 - 1) \tag{22}$$

2.4 Wavefront Correction

To correct the wavefront, we needed to calculate the correcting phase that will serve as the input to the SLM. The capability of the SLM for wavefront shaping was demonstrated in the photopolymerization of microgear patterns by encoding in the SLM the topological charge and phase level of an optical vortexp (G. Bautista and Daria, 2009). Another work uses the SLM to reshape light in three dimensions (P.L.A. Hilario and Tapang, 2014). This makes it possible to correct the aberrations inherent to the telescope. The phase information from intensity image was retrieved using the Gerchberg-Saxton (GS) algorithm. From the intensity image of the PSF, the amplitudes of the

input data can be obtained by taking the square root of the measured intensities (Goodman, 2005).

$$U(x,y) = \sqrt{I(x,y)}exp(i\phi(x,y)) \quad (23)$$

Using Equation 23, we first take a guess phase $\phi(x,y)$. We multiply this phase to the amplitude of the source image and take the Fourier transform. We take the phase of the resulting complex field and multiply it with the amplitude of the target image. We get the inverse Fourier transform and check if the target image has already been reconstructed. This procedure is repeated until a tolerable reconstruction error is obtained (R.W. Gerchberg, 1972). A diagram of the algorithm is shown in Figure 4.

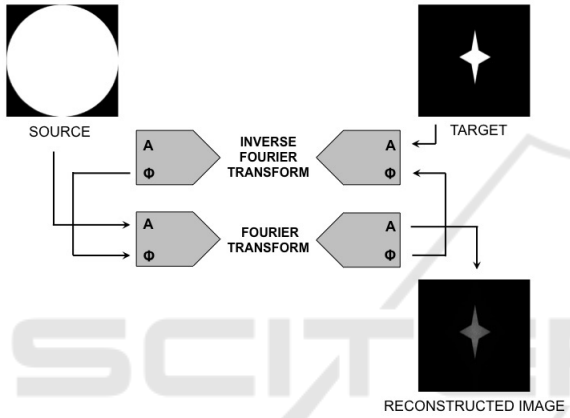

Figure 4: Schematic of the GS algorithm.

For our simulations, we used aberrated PSF of the segmented mirror as our source and the unaberrated PSF of the segmented mirrors as the target. The phase information retrieved using the GS algorithm serves as the correction phase. To check if the correction successful, we denote the correction phase as $\Phi_{correction}$ and use Equation 24.

$$PSF_{corrected} = \mathcal{F}\{|\mathcal{F}^{-1}\{PSF_{aberrated}\}|exp(i\Phi_{correction})\} \quad (24)$$

The quality of the reconstruction is evaluated using the Linfoot's criteria of merit given by Equation 27. When all these values are 1, it means that the signal was perfectly recovered. If C <1, the reconstructed profile is narrower than the target profile. When Q <1, it means that the reconstructed and target profiles are erroneously close to each other (G.Tapang and Saloma, 2002).

$$F = 1 - \frac{<(I_{target} - I_{reconstructed})^2>}{<(I_{target})^2>} \quad (25)$$

$$Q = \frac{<(I_{reconstructed})^2>}{<(I_{target})^2>} \quad (26)$$

$$C = \frac{<|I_{reconstructed}||I_{target}|>}{<(I_{reconstructed})^2>} \quad (27)$$

3 RESULTS AND DISCUSSION

Figure 5 shows the transverse PSFs of a single mirror segment, the segmented mirrors and the monolithic mirror. Adding the fields due to the 7 mirrors, we get a PSF that is much smaller than the individual mirror segment. This is expected since the effective aperture diameter of the segmented mirrors is now larger than a single mirror.

Taking the cross-section of the PSFs, we see that the width of the Airy disk of the segmented mirror is broader than that of the monolithic mirror despite having the same aperture diameter. This is due to the segmentation of the reflecting telescope.

Figures 6 and 7 show the results of the aberration correction. Using the GS algorithm, the added aberrations were corrected. The quality of the correction is evaluated by computing the Linfoot's criteria of merit values of both the aberrated PSF and the corrected PSF as shown in Table 1.

The SLM in Figure 1 is a transmitting twisted nematic spatial light modulator such as the Holoeye LC2012. Modulation in phase occurs when an electric field is applied causing the molecules to align themselves along its direction. The correcting phase obtained using the GS algorithm will be sent to the SLM via a video signal from the computer. In the actual experiment, the PSF should be scaled such that $\triangle f = \frac{\lambda f M}{a}$ where λ is the wavelength, f is the focal length, M is equal to the pixel dimension and a is the aperture diameter. We computed $\triangle f$ to be equal to $640\mu m$.

The use of identical mirrors reduces the cost and complexity in constructing telescopes with very large apertures. It eliminates the need to precisely shape the mirrors which requires each mirror segment to be polished well up to the edge in order to seamlessly form one large mirror. Thus, increasing the quantity production of the mirrors. Mounting the mirror will also be easier since the structural support will not depend on the individual shape of the mirror segments. Furthermore, placing an adaptive optics device, such as the SLM, before the camera allows the incoming wavefront to be shaped to compensate for any mis-

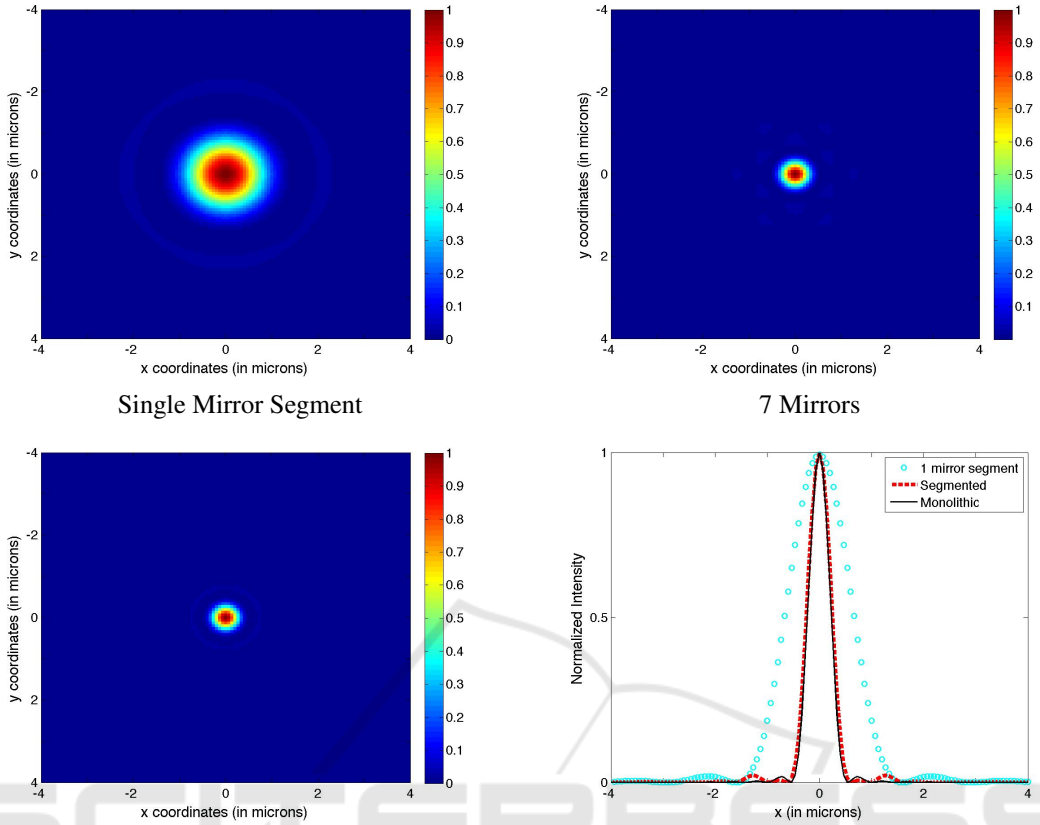

Figure 5: PSFs of a single mirror segment, segmented mirror and the monolithic mirror.

Table 1: Linfoot's criteria of merit for aberrated and the corrected PSF using the angular spectrum method.

Aberration		Fidelity	Structural Content	Correlation
Spherical Aberration	Aberrated	0.9670	0.7005	0.8337
	Corrected	1.0000	1.0000	0.9988
Coma	Aberrated	0.9956	0.9990	0.9973
	Corrected	1.0000	1.0000	1.0000
Astigmatism	Aberrated	0.0179	0.0137	0.0158
	Corrected	0.9843	1.0000	0.9922
Defocus	Aberrated	0.0045	0.0022	0.0033
	Corrected	0.9843	1.0000	0.9922

alignment and aberrations inherent in the telescope system.

4 CONCLUSION AND RECOMMENDATION

We have demonstrated a technique to correct aberrations in a basic segmented reflecting telescope by using the GS algorithm to obtain the correction phase. We have numerically evaluated the technique and have shown that it was able to reduce the effects of aberrations. Using this technique, we remove the need for shaping of the individual mirror segments precisely. The intensity of the side lobes in the PSF due to errors in alignment can be compensated using a single SLM. The wavefront can be shaped such that the imaging resolution can be improved to make it at par with the performance of one large mirror.

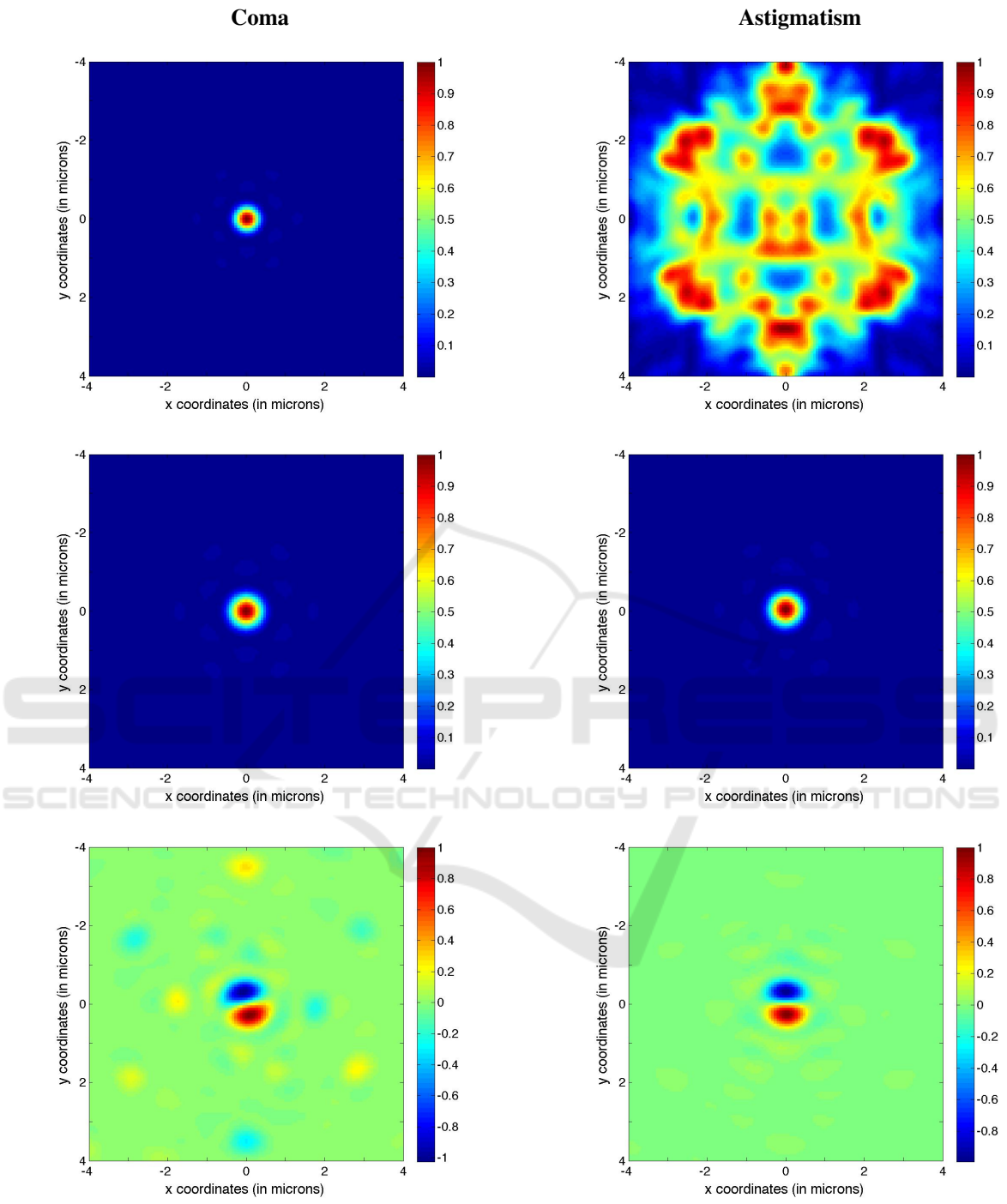

Figure 6: Aberrated (1st row), corrected (2nd row) and the difference between the target and the corrected PSF of the segmented reflecting telescope.

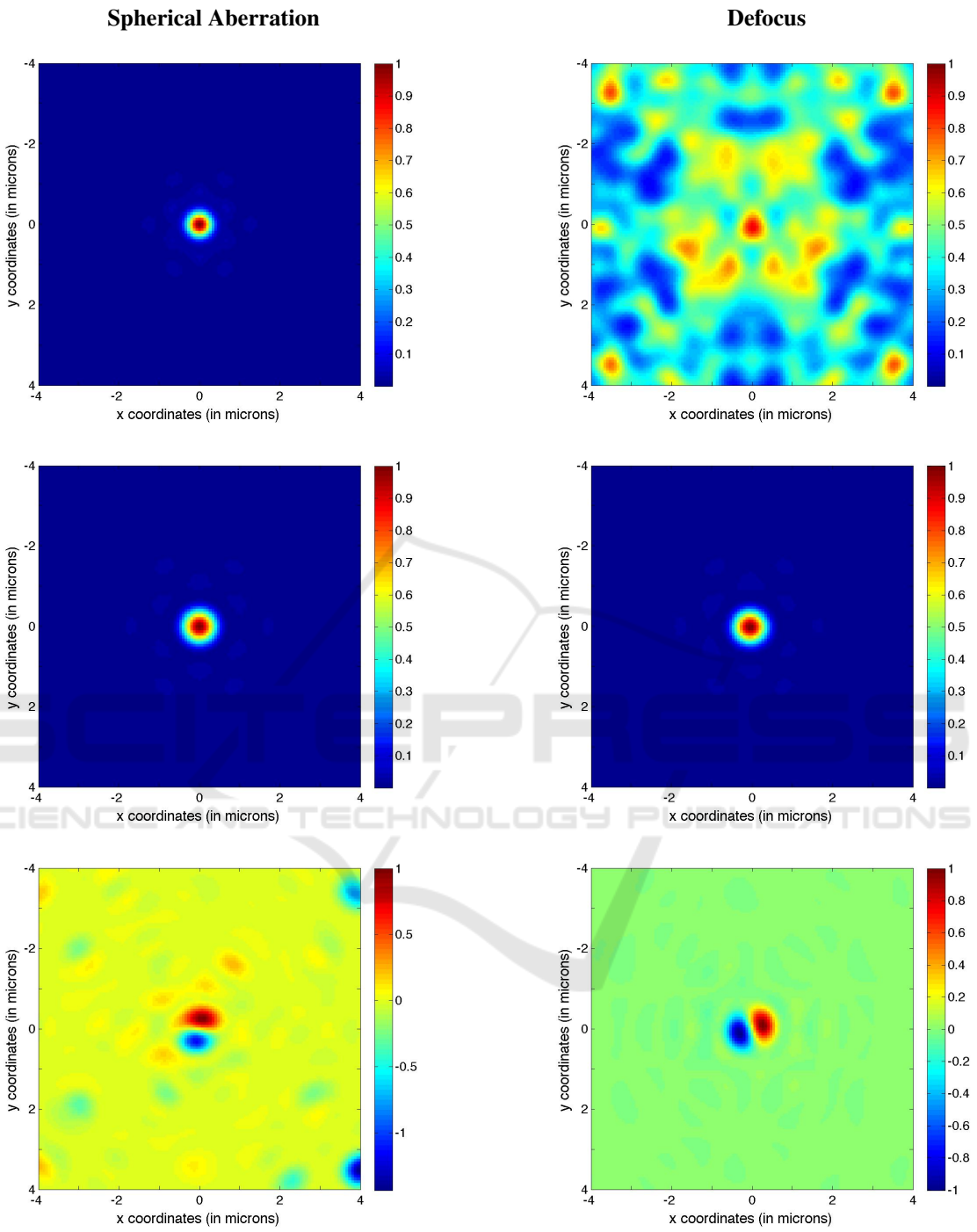

Figure 7: Aberrated (1st row), corrected (2nd row) and the difference between the target and the corrected PSF of the segmented reflecting telescope.

REFERENCES

G. Bautista, M.J. Romero, G. T. and Daria, V. (2009). Parallel two-photon photopolymerization of microgear patterns. *Optics Communications*, 282(18):3746–3750.

G. Chanan, J. Nelson, T. M. (2013). Semented mirror telescopes. In *Planets, Stars and Stellar Systems*, volume Volume 1: Telescope and Instrumentation, pages 99–136. Springer.

Goodman, J. (2005). *Introduction to Fourier Optics*. Roberts and Compan Publishers, 3rd edition.

G.Tapang and Saloma, C. (2002). Behavior of the point-spread function in photon-limited confocal microscopy. *Applied Optics*, 41(8):1534–1540.

M. Born, R. W. (1999). *Principle of Optics*. Cambridge University Press.

Mahajan, V. (1994). Zernike circle polynomials and optical aberrations of systems with circular pupils. *Supplement to Applied Optics*, pages 8121–8124.

P.L.A. Hilario, M. V. and Tapang, G. (2014). Independent light fields generated using a phase only spatial light modulator. *Optics Letters*, 39(7):2036–2039.

R.W. Gerchberg, W. S. (1972). A practical algorithm for the determination of phase from image and diffraction plane pictures. *Optik*, 35(2):237–246.